Simulating a Brownian type of motion: The rescaling-velocity approach versus the Langevin approach

E. Barkai and V. Fleurov
Beverly and Raymond Sackler School of Physics and Astronomy, Tel Aviv University, Tel Aviv 69 978, Israel
(Received 21 October 1994)

The dynamics of a classical test particle that evolves deterministically in a potential field, and whose velocity is then randomized at regular intervals of time, is discussed. A limiting procedure for this type of Brownian type of motion is given, which results in a motion like that described by the Langevin equation. Exact analytical solutions for free and harmonically bound particles are obtained. It is shown that if the time intervals between randomizing events coincide with the period of harmonic oscillations, thermal equilibrium is not reached. For anharmonic background potentials such a resonant behavior also shows up as a slowing down of the relaxation.

PACS number(s): 05.40.+j, 02.50.Ng, 02.60.−x

I. INTRODUCTION

One of the ways to simulate numerically the dynamics of a system in contact with a heat bath is given by the so-called rescaling-velocity (RV) approach. A test particle of mass M moves according to Newton's law of motion (without friction) in an external potential. Then at regular time intervals τ_0 the particle is stopped and its momentum is reset to a new random value chosen from a Gaussian distribution with variance k_BTM (T is the bath temperature and k_B is the Boltzmann constant). Such an event will be called below a collision. It is important to emphasize that the time scale τ_0 may be comparable with the time scales of the background potential. Using the reasoning of detailed balance it was shown that the test particle distribution will become the Boltzmann distribution [1].

The algorithm, briefly outlined here, is sometimes also called the stop-start mechanism. It is used to simulate many particle systems. It finds its application in such diverse fields as lattice gauge theories [1], condensed matter physics [2], chemical reaction rates [3,4], and chaos theory [5]. On some occasions the time interval τ_0 is chosen from an exponential distribution. The RV approach is an alternative both to the celebrated Monte Carlo (MC) and to the Langevin approach. In the latter case both a friction force and noise act on the test particle.

Recently Duane *et al.* [1], in the context of lattice field theory, have proposed a hybrid Monte Carlo (HMC) approach in which every RV collision is followed by the Metropolis accept-reject procedure. This algorithm reduces to the RV approach if the discretization errors are of minor importance. The HMC algorithm has the advantage of being stable and not sensitive to the chosen discretization time step Δt. This method was used by Mehling *et al.* [6] for simulating condensed matter systems. Clearly the method suggested by Duane *et al.* is a promising alternative to the MC, Langevin, and RV approaches.

Such a broad application of the RV approach inspired us to use it for a broader class of stochastic dynamics and study it possibly analytically. Our first aim is to find the RV dynamics for some simple cases and compare it with the diffusion limit where much numerical [7,8] and analytical [9] work is done. The conventional RV approach resembles to an extent the Rayleigh piston model [9,10] for equal masses of colliding particles. It is treated here analytically for the case of a general ratio of masses for some simple cases. The relaxation and fluctuation patterns of this mechanism are compared with the diffusion limit results. For example, it is found that the relaxation in a harmonic field is not characterized by a single transition from overdamped to underdamped motion but rather an infinite number of such transitions are found. We have also found under what conditions the RV approach will produce the same dynamical results as described by the Langevin equation, thus establishing a method to simulate the diffusion limit.

In the special case when the time τ_0 equals an integer number of the harmonic oscillator period the RV algorithm does not produce a relaxation of the test particle to the thermal equilibrium. This is rather unexpected since the detailed balance is not violated in this case. This is a clear indication of a violation of the ergodic hypothesis. Considering numerically an anharmonic oscillator an analogous effect is revealed. It shows up in this case as a slowing down of the relaxation when τ_0 is close to the thermally averaged period of the test particle motion.

We have also checked the stability of the stochastic paths when changing the computer discretization Δt. We have found a sharp transition between states where trajectories are stable and unstable. This transition occurs when varying τ_0 from short (stable) to long (unstable) periods.

The paper is organized as follows. First we present the model and the mathematical tools we use for solving the problem. We then solve the model for the special cases of the free particle and the particle in a harmonic field. After this the case of a general potential is considered

and it is shown that the RV evolution of the system in the diffusion limit is described by the Kramers equation. The last section investigates numerically the motion of the test particle in an anharmonic potential. It is shown how the procedure leads to the equilibration of the test particle and the case of the relaxation slowing down is discussed. Then the stability of the random paths is discussed.

II. MODEL

This section considers a simple, one-dimensional model for a system coupled with a bath (i.e., a random number generator). Let us assume that a test particle with the mass M moves in the potential $V(x)$. Its motion is described by the Newton equation. The particle may interact with a bath which is a one-dimensional gas of other particles with the mass m. After each interval τ_0 the reference particle is elastically kicked by a gas particle with a momentum $\tilde{p}$ whose values are distributed according to the Maxwell function with a variance k_BTm. Such an event causes a change of the momentum of the reference particle described by the equation

$$p^+ = \mu_1 p^- + \mu_2 \tilde{p},$$

where

$$\mu_1 = \frac{M-m}{M+m}, \quad \mu_2 = \frac{2M}{M+m}.$$

Here $-$ and $+$ mark the values of the momentum just before and after the collision. The coordinate of the reference particle does not change in the course of the collision.

Now a sequence $\{\tilde{p}_i\}$ of k collision events is considered. The equation of motion and the elastic character of the collisions in principle give the possibility to find the coordinate x_k and momentum p_k of the test particle just after the kth collision. It is clear that these two quantities depend on their initial values x_0 and p_0 and the particular choice of the sequence $\{\tilde{p}_i\}$ and they are denoted as $x_k(\{\tilde{p}_i\}; x_0, p_0)$ and $p_k(\{\tilde{p}_i\}; x_0, p_0)$.

It is useful for further application to define the characteristic function

$$C_k(l,h,T;x_0,p_0) = \langle \exp\{ix_k l + ip_k h\}\rangle = \underbrace{\int\cdots\int}_{k \text{ integrations}} \prod_{i=1}^{k} \frac{d\tilde{p}_i}{\sqrt{2\pi mT}} \exp\left\{-\frac{\tilde{p}_i^2}{2mT}\right\} \exp\left[ix_k(\{\tilde{p}_i\};x_0,p_0)l + ip_k(\{\tilde{p}_i\};x_0,p_0)h\right]. \tag{1}$$

The second line of Eq. (1) explains the meaning of the averaging procedure denoted by the brackets $\langle\,\rangle$.

The characteristic function (1) allows for the direct calculation of various moments of the test particle coordinate and momentum. The following two subsections consider two cases when the characteristic function (1) can be calculated exactly.

A. Free particle

The simplest case we are going to consider corresponds to the free particle in the sense that there is no force acting on it. However, it is not free from interaction with the bath. We assume also that the collisions follow one after another after a constant time τ_0. In this case one can readily write the recursion

$$\begin{aligned} x_{k+1} &= x_k + \frac{p_k^+ \tau_0}{M}, \\ p_{k+1}^+ &= \mu_1 p_k^+ + \mu_2 \tilde{p}_{k+1}, \end{aligned} \tag{2}$$

connecting the coordinate and the momentum of the test particle after the kth and $(k+1)$th collision. The map (2) results in the equation

$$\begin{aligned} x_k &= \frac{\tau_0}{M}\sum_{i=0}^{k-1}\mu_1^i p_0 + \mu_2 \frac{\tau_0}{M}\sum_{i=1}^{k-1}\sum_{j=i}^{k-1}\mu_1^{j-i}\tilde{p}_i, \\ p_k^+ &= \mu_1^k p_0 + \sum_{i=1}^{k}\mu_1^{k-i}\mu_2\tilde{p}_i. \end{aligned} \tag{3}$$

Here without a loss of generality $x_0 = 0$. Now (3) can be substituted into Eq. (1) for the characteristic function. Carrying out all the Gaussian integrations of the bath particle momenta $\tilde{p}_i$ one arrives at the equation

$$C_k(l,h,T;x_0,p_0) = C_k^0 \exp\left(-\frac{h^2MT}{2}(1-\mu_1^{2k})\right)\exp\left(-\frac{hl\tau_0\mu_1 T}{1-\mu_1}[1-\mu_1^k-\mu_1^{k-1}+\mu_1^{2k-1}]\right)$$

$$\times \exp\left(-\frac{Tl^2\tau_0^2(1+\mu_1)}{2M(1-\mu_1)}\left[k+\frac{2\mu_1^k}{1-\mu_1}-\frac{\mu_1^{2k}}{1-\mu_1^2}-\frac{1+2\mu_1}{1-\mu_1^2}\right]\right) \tag{4}$$

for the characteristic function, in which the factor

$$C_k^0 = \exp\left[ih\mu_1^k P_0 + \frac{il\tau_0 P_0(1-\mu_1^k)}{M(1-\mu_1)}\right] \tag{5}$$

absorbs all the dependence on the initial conditions.

The characteristic function (4) is defined only for discrete values of time, $k\tau_0$, but the calculation of this function between the kth and the $(k+1)$th collision does not present a serious problem since the Newton equation of motion can be readily solved. It is easy to check that the momentum of the test particle equilibrates to the Maxwell distribution. The motion is unlimited; hence no normalized distribution exists for the coordinate of the test particle. In the next subsection the harmonic oscillator will be considered whose potential restricts the motion of the test particle in a certain region, and this problem does not take place.

Now various moments of the coordinate and momentum are produced by differentiating the characteristic function (4) over h or l and taking the limit $h, l \to 0$. Several first moments are listed below:

$$\langle p\rangle = p_0 e^{-\gamma t}, \tag{6a}$$

$$\langle x\rangle = \frac{\tau_0 P_0}{M}\frac{1+\varepsilon}{2\varepsilon}(1-e^{-\gamma t}), \tag{6b}$$

$$\langle p^2\rangle = p_0^2 e^{-2\gamma t} + MT\left(1-e^{-2\gamma t}\right), \tag{6c}$$

$$\langle xp\rangle = \langle x\rangle\langle p\rangle + \frac{\tau_0 T(1-\varepsilon)}{2\varepsilon} \times\left[1-\frac{2}{1-\varepsilon}e^{-\gamma t}+\frac{1+\varepsilon}{1-\varepsilon}e^{-2\gamma t}\right], \tag{6d}$$

$$\langle x^2\rangle = \langle x\rangle^2 + \langle x_d^2\rangle, \tag{6e}$$

$$\langle x_d^2\rangle = \frac{\tau_0^2 T}{\varepsilon M}\left[\frac{t}{\tau_0}+\frac{\varepsilon+1}{\varepsilon}e^{-\gamma t}-\frac{(1+\varepsilon)^2}{4\varepsilon}e^{-2\gamma t} -\frac{(3-\varepsilon)(1+\varepsilon)}{4\varepsilon}\right]. \tag{6f}$$

Here

$$\varepsilon = \frac{m}{M}, \quad \gamma = \frac{1}{\tau_0}\ln\frac{1+\varepsilon}{1-\varepsilon}. \tag{7}$$

Equation (6a) describes the deceleration of the test particle with the initial momentum p_0. It is clear that γ is the friction coefficient. Even so the relaxation of the first moment is not continuous due to the free motion between the collision events. The average squared momentum (6c) relaxes to TM with the relaxation constant of 2γ. This kind of relaxation is identical to the relaxation with a continuous friction force and a fluctuating force as described by the Langevin equation [9].

The mean square displacement (6e) contains two terms. The first one depends essentially on the initial momentum of the test particle and corresponds to the displacement of the particle before its initial momentum is completely damped. The second term (6f) describes diffusion and increases linearly with time in the limit $t \to \infty$. The corresponding diffusion coefficient can be easily found:

$$D = \frac{\tau_0 T}{2M\varepsilon}.$$

It is important to emphasize that the Einstein relation does not generally hold for this system since $D \neq T/\gamma M$. This is connected with the fact that we consider finite time intervals τ_0 between the collisions and finite ratio ε of the masses. As a result the relaxation time appears to be comparable with this time interval. Therefore the relaxation is not a continuous process but rather occurs in a small number of steps. No wonder that the Einstein relation assuming slow and continuous relaxation does not hold under these conditions.

In order to recover the Einstein relation one has to take the continuous limit $\tau_0 \to 0$. Taken as it is this limit means increasing frequency of collisions and hence increasing friction. In order to have a finite friction coefficient one must simultaneously take the limit $\varepsilon \to 0$ keeping the ratio $\gamma_L = 2\varepsilon/\tau_0$ finite. Then one can readily see that

$$\gamma \to \gamma_L = \frac{T}{DM},$$

i.e., the Einstein relation is now valid.

This limit produces the mean square displacement

$$\langle x^2\rangle = \left(\frac{p_0}{\gamma_L M}\right)^2\left(1-e^{-\gamma_L t}\right)^2 + \frac{T}{\gamma_L^2 M}\left[2t\gamma_L - 3 + 4e^{-\gamma_L t} - e^{-2\gamma_L t}\right], \tag{8}$$

which coincides with the well-known solution of the Langevin equation with the friction coefficient γ_L. In the same way all the moments listed above approach the solutions of the Langevin equation. That is why we shall call, in what follows, the above limit the Langevin (or the diffusion) limit.

B. Harmonic oscillator

The stochastic motion of the particle in a harmonic oscillator is considered in this subsection. This problem can also be analyzed exactly due to the fact that the evolution of the coordinate and the momentum is described by the linear map

$$\begin{pmatrix}\tilde{x}_{k+1}\\ p_{k+1}^+\end{pmatrix} = \begin{pmatrix}\cos(\omega\tau_0) & \sin(\omega\tau_0)\\ -\mu_1\sin(\omega\tau_0) & \mu_1\cos(\omega\tau_0)\end{pmatrix}\begin{pmatrix}\tilde{x}_k\\ p_k^+\end{pmatrix} + \begin{pmatrix}0\\ \mu_2\tilde{p}_{k+1}\end{pmatrix}, \tag{9}$$

where $\tilde{x}_k = M\omega x_k$. The matrix in Eq. (9) does not depend on the coordinate and momentum of the test par-

ticle, which allows one to carry out a procedure similar to that of the previous section.

This matrix is diagonalized and Eq. (9) becomes

$$\begin{pmatrix} \theta_{k+1} \\ \vartheta_{k+1} \end{pmatrix} = \begin{pmatrix} E_- & 0 \\ 0 & E_+ \end{pmatrix} \begin{pmatrix} \theta_k \\ \vartheta_k \end{pmatrix} + \begin{pmatrix} -\mu_2 a_+ \tilde{p}_{k+1} \\ \mu_2 a_- \tilde{p}_{k+1} \end{pmatrix} \tag{10}$$

where

$$E_\pm = \frac{1}{2}\Big[\cos(\omega\tau_0)(1+\mu_1) \pm \sqrt{\cos^2(\omega\tau_0)(1+\mu_1)^2 - 4\mu_1}\Big] \tag{11}$$

and

$$\theta_k = b_+\tilde{x}_k - a_+ p_k, \qquad \vartheta_k = -b_-\tilde{x}_k + a_- p_k. \tag{12}$$

The coefficients in Eq. (12) make two eigenvectors of the matrix in Eq. (9).

Now assuming initial values θ_0 and ϑ_0 and a given sequence of k incident particle momenta $\{\tilde{p}_i\}$ with $i = 1, 2, \ldots, k$ Eq. (12) results in

$$\theta_k = E_-^k\theta_0 - \mu_2 a_+ \sum_{i=1}^{k} E_-^{i-1}\tilde{p}_{k-i+1}, \qquad \vartheta_k = E_+^k\vartheta_0 + \mu_2 a_- \sum_{i=1}^{k} E_+^{i-1}\tilde{p}_{k-i+1}. \tag{13}$$

The characteristic function for the k collision process

$$C_k(l_1, l_2, T; \theta_0, \vartheta_0) = \langle e^{il_1\theta_k + il_2\vartheta_k}\rangle \tag{14}$$

is calculated by integrating over all the incident momenta $\tilde{p}_i$ with the Maxwell distribution. The result can be represented in the form (for $\tau_0\omega \neq n\pi$ with integer n)

$$C_k(l_1, l_2, T; \theta_0, \vartheta_0) = C_0(\theta_0, \vartheta_0)\tilde{C}_k(l_1, l_2, T; \theta_0, \vartheta_0), \tag{15}$$

where

$$C_0(l_1, l_2; \theta_0, \vartheta_0) = \exp(i[l_1 E_-^k\theta_0 + l_2 E_+^k\vartheta_0])$$

contains the dependence on the initial conditions

$$\tilde{C}_k(l_1, l_2, T) = \exp\left\{-\frac{1}{2}\mu_2^2 mT f_k(l_1, l_2)\right\},$$

$$f_k(l_1, l_2) = (a_+l_1)^2\frac{1-E_-^{2k}}{1-E_-^2} + (a_-l_2)^2\frac{1-E_+^{2k}}{1-E_+^2} - 2a_+a_-l_1l_2\frac{1-(E_-E_+)^k}{1-E_-E_+}. \tag{16}$$

This result is considered first in the large time limit which corresponds to $k \to \infty$ when one expects that the system must tend to equilibrium. Really the factor $C_0(l_1, l_2; \theta_0\vartheta_0)$ depending on the initial conditions tends to unity in this limit, while the characteristic function (16) at $k \to \infty$ reads

$$C_k(l_1, l_2, T) = \exp\left\{-\frac{1}{2}\mu_2^2 mT\left[\frac{(a_+l_1)^2}{1-E_-^2} + \frac{(a_-l_2)^2}{1-E_+^2} - \frac{2a_+a_-l_1l_2}{1-E_-E_+}\right]\right\}. \tag{17}$$

One can also carry out direct averaging using the equilibrium Maxwell-Boltzmann distribution. The result coincides with (17). It is important to emphasize that the two averaging procedures are different. The first one (17) just follows all histories of the system and does not involve any phase space averaging. The second procedure, on the contrary, is phase space averaging of the test particle. If the ensemble average does not coincide with the averaging over the incident particles' momenta, it is a clear indication that the ergodicity is broken. Such cases will be considered in the next subsection.

The quantities of greatest interest are the first and second moments of the coordinate and mechanical momentum $\langle x\rangle$, $\langle p\rangle$, $\langle x^2\rangle$, and $\langle p^2\rangle$, which can be found as corresponding linear combinations of the moments $\langle\theta\rangle$, $\langle\vartheta\rangle$, $\langle\theta^2\rangle$, $\langle\vartheta^2\rangle$, and $\langle\theta\vartheta\rangle$ obtained from the characteristic function (16):

$$\langle x\rangle = \frac{1}{(1+E_+E_-)(E_+-E_-)}\left\{x_0[(E_+^2-1)E_-^{k+1} - (E_-^2-1)E_+^{k+1}] - \frac{p_0}{M\omega}\sqrt{(1-E_-^2)(1-E_+^2)}(E_-^k - E_+^k)\right\},$$

$$\langle p\rangle = \frac{1}{(1+E_+E_-)(E_+-E_-)}\left\{M\omega x_0 E_-E_+\sqrt{(1-E_+^2)(1-E_-^2)}(E_-^k - E_+^k) + p_0[E_-(E_+^2-1)E_+^k - E_+(E_-^2-1)E_-^k]\right\}, \tag{18}$$

$$\langle x^2\rangle = \langle x\rangle^2 + \frac{T}{M\omega^2}\left\{1 - \left[\frac{1}{(1+E_-E_+)(E_+-E_-)^2}[(1-E_+^2)(1-E_-E_+)E_-^{2k} + (1-E_-^2)(1-E_-E_+)E_+^{2k} - 2(1-E_-^2)(1-E_+^2)(E_-E_+)^k]\right]\right\},$$

$$\langle p^2\rangle = \langle p\rangle^2 + TM\left\{1 - \left[\frac{1}{(1+E_-E_+)(E_+-E_-)^2}[E_+^2(1-E_-^2)(1-E_-E_+)E_-^{2k} + E_-^2(1-E_+^2)(1-E_-E_+)E_+^{2k} - 2E_+E_-(1-E_-^2)(1-E_+^2)(E_-E_+)^k]\right]\right\}. \quad (19)$$

The absolute values of both eigenvalues (11) are smaller than 1 and the time dependences of the moments (18) and (19) are characterized by two parameters

$$\gamma_\pm = -\frac{1}{\tau_0}\ln(E_\pm) \quad (20)$$

appearing in the dependences

$$E_\pm^k = \exp(-t\gamma_\pm).$$

The decay parameters (20) have or do not have an imaginary part depending on the sign of the quantity $\Delta = \cos^2(\omega\tau_0)(1+\mu_1)^2 - 4\mu_1$ in Eq. (11), which depends on two parameters $\tau_0\omega$ and μ_1. The parameter μ_1 varies for different masses of the test and bath particles from -1 to 1. Δ is negative only if

$$1 \geq \mu_1 > \mu_1^* = 2\frac{1-|\sin\tau_0\omega|}{\cos^2\tau_0\omega} - 1.$$

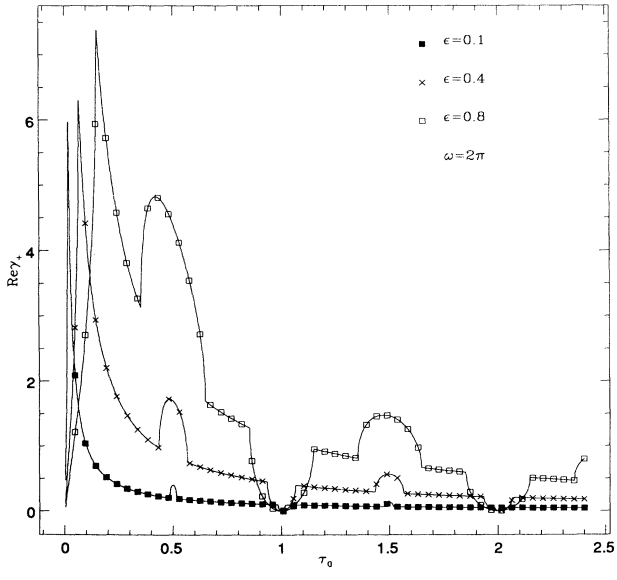

FIG. 1. $\mathrm{Re}\gamma_+$ versus τ_0 for different mass ratios ε. To the right of the first peak $\mathrm{Re}\gamma_+$ is determined (not including the blips) by the damping coefficient of the free particle. Blips appear when E_+ is real. For $\omega\tau_0 = 2\pi n$, $\mathrm{Re}\gamma_+ = 0$.

In this case

$$\gamma_\pm = -\frac{1}{2\tau_0}\ln\mu_1 \pm i\theta, \quad (21)$$

where

$$\theta = \frac{1}{\tau_0}\arctan\left(\sqrt{\frac{|\Delta|}{4\mu_1+\Delta}}\right).$$

Therefore we have here a type of underdamped behavior when the system oscillates with the frequency θ, while the amplitude of these oscillations decays with the characteristic decay time $-2\tau_0/\ln\mu_1$. One can readily see (7) that this time is twice as large as the decay time obtained in the previous subsection for the motion of a free particle.

If $\mu_1^* \geq \mu_1 \geq 0$ and both eigenvalues $E_\pm$ are real and positive we deal with a type of overdamped behavior of the system when no oscillations take place (see Figs. 1–3). This does not prevent the particle from exploring the phase space, since the particle oscillates with the frequency ω between the collision events. In this case the

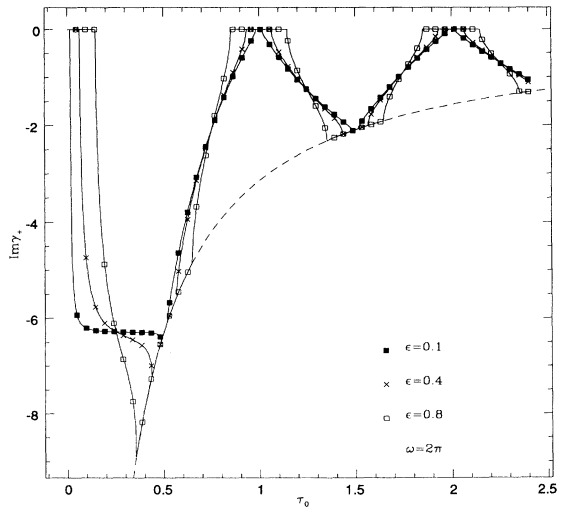

FIG. 2. $\mathrm{Im}\gamma_+$ versus τ_0 for different mass ratios ε. The dashed line shows the dependence of $-\frac{\pi}{\tau_0}$ which holds when $E_+ < 0$.

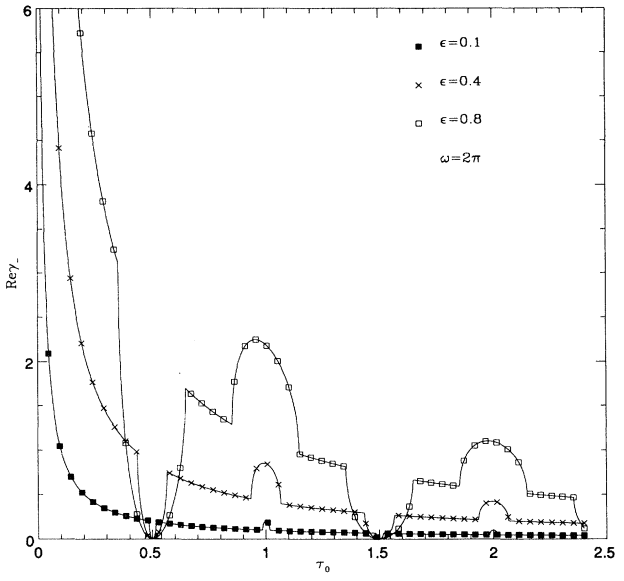

FIG. 3. $\mathrm{Re}\gamma_-$ versus τ_0 for different mass ratios ϵ for $\lim_{\tau_0\to 0}\mathrm{Re}\gamma_- = \infty$. Blips appear when E_- is real except for small values of $\tau_0 \to 0$ when the motion is overdamped. For γ_- we have $\mathrm{Im}[\gamma_-] = -\mathrm{Im}[\gamma_+]$.

relaxation does not depend only on the damping coefficient of the free particle and the frequency of the oscillator. It rather depends on three parameters which may be, for example, chosen as (μ_1, ω, τ_0).

When E_+ or $E_- < 0$, a special behavior of the particle is revealed. In this case the first moment of the normal coordinates, which may be computed directly from (13) and given by $\langle \vartheta_k \rangle = \vartheta_0 E_+^k$, $\langle \theta_k \rangle = \theta_0 E_-^k$, changes sign after each collision. When this happens, the points in the θ, ϑ plane where the collisions occur alternate between different sectors (quarters). Such a behavior does not appear in the Langevin limit, when $E_\pm$ may become complex but are never real negative numbers due to the continuous nature of the collisions in this limit.

This may happen when $\Delta > 0$, $\cos(\omega\tau_0) < 0$, $\mu_1 > 0$, then $E_\pm < 0$. In this case one may consider directly the coordinates x, p. As an example, when $p_0 = 0$, $\langle x \rangle$ changes sign after each collision. Hence collisions occur once to the left and then to the right of the central point of the oscillator.

Another interesting situation appears when $\mu_1 = E_+E_- < 0$. The eigenvalues $E_\pm$ are real but have different signs, E_+ remaining positive while E_- becomes negative. This corresponds to a rather unusual case when the mass of the bath particle is larger than the mass of the test particle. This situation is certainly very far from those considered by conventional theories of diffusive motion where the bath particles are usually assumed to be very light. However, the solution presented in this subsection does not contain any restrictions on the ratio of masses and heavy bath particles may also be considered. The hopping from sector to sector seems to be a result of light test particles being elastically reflected by the heavy bath particles. Then each collision strongly changes the further motion of the test particle.

Special cases

The first special case which is considered here is the situation of equal masses $M = m$, which means that $\mu_1 = 0$. Now one of the eigenvalues becomes zero, $E_- = 0$, and the corresponding relaxation time $\tau_- = 1/\gamma_-$ also becomes zero. This is the case used in the standard RV algorithm. Two colliding particles of equal masses simply exchange their momenta (in one dimension). Therefore the momentum distribution of the test particle coincides with that of the bath particle just after the first collision and, for example, $\langle p \rangle = 0$ for any value of $k \neq 0$.

This consideration being sufficient for the free particle should be additionally elaborated, since now there is a potential acting on the test particle. Its influence shows up in the second relaxation time $\tau_+ = -\tau_0/\ln[\cos(\tau_0\omega)]$ which leads to the following equations for the moments for $k > 0$:

$$\begin{aligned} \langle x \rangle_k &= \left[x_0 + \frac{p_0}{M\omega}\tan(\tau_0\omega)\right]\cos^k(\tau_0\omega), \\ \langle x^2 \rangle_k &= \langle x \rangle_k^2 + \frac{T}{M\omega^2}[1 - \cos^{2k-2}(\tau_0\omega)], \\ \langle p^2 \rangle &= MT, \qquad \langle p \rangle = 0. \end{aligned} \tag{22}$$

In the large time limit ($t = k\tau_0 \to \infty$) all the moments relax to their equilibrium values with the finite relaxation time τ_+. When $\tau_0 \to 0$ the particle is strongly overdamped and the motion is practically frozen.

A really special case is achieved when $\tau_0\omega = n\pi$, where n is an integer number. Then $E_+ = 1$ or $E_- = -1$ and both $\mathrm{Re}\gamma_+ = 0$ and $\mathrm{Re}\gamma_- = 0$ (see Figs. 1 and 3) meaning that real equilibrium is not achieved at all. To see this one can write the moments in the $k \to \infty$ limit:

$$\begin{aligned} |\langle x \rangle| &= x_0, \qquad \langle p \rangle = 0, \\ \langle x^2 \rangle &= x_0^2, \qquad \langle p^2 \rangle = TM. \end{aligned} \tag{23}$$

The system does not "forget" the initial coordinate, contrary to the initial momentum which does not appear in Eq. (23).

This property can be understood rather easily. The particle in the harmonic potential visits the point where it has started its motion with a period independent of the amplitude of the oscillations. The bath particles collide with the test particle also periodically, and if these two periods coincide, or their ratio is an integer number, then the periodic motion of the harmonic oscillator is not disturbed. The collisions occur always when the test particle visits the same point and they result only in random fluctuations of the amplitude of the harmonic oscillations, while the phase is not randomized. When the period of the oscillator is twice as long as the mean time between collisions, the collisions will occur at two special points, x_0 and $-x_0$, again leading to no relaxation. In both these cases the energy of the harmonic oscillator will always be larger than $E_{min} = M\omega^2 x_0^2/2$ for any low temperature.

To complete the discussion of this section we present

here results for the Langevin limit which is achieved if $\varepsilon \to 0$, $\tau_0 \to 0$ under the condition that $\gamma_L = 2\varepsilon/\tau_0$ remains finite. Then the two relaxation times are

$$\frac{1}{\tau_\pm} = \lim_{\substack{\varepsilon \to 0 \\ \tau_0 \to 0}} \gamma_\pm = \frac{1}{2}(\gamma_L \mp \sqrt{\gamma_L^2 - 4\omega^2}).$$

Taking this limit in Eqs. (18) and (19) one arrives at the results obtained by Chandrasekhar [11], who treated a particle described by the Langevin equation and bounded by a harmonic force field.

III. KRAMERS EQUATION

Two simple cases of a free particle and a harmonic oscillator interacting with the bath as described above allow for exact solutions for any values of the parameters. Now we are going to address the more general case of a particle moving in an arbitrary smooth potential $V(x)$. We are not able to find an exact solution of this problem. However, there is a possibility to describe the time evolution of the characteristic function by an equation which in the continuous limit ($\tau_0, \varepsilon \to 0$) coincides with the Kramers equation. The derivation is similar to the Feynman derivation [12] of the Schrödinger equation from the path integral formalism of quantum mechanics.

As usual we consider the time τ_0 between the collisions as constant and also small enough to ensure the expansion

$$\hat{x}_{k+1} = x_k + \frac{p_k^+}{M}\tau = x_k + \left(\frac{\mu_1 p_k^- + \mu_2 \tilde{p}_k}{M}\right)\tau, \tag{24}$$

$$\hat{p}_{k+1} = p_k^+ + f(x_k)\tau = \mu_1 p_k^- + \mu_2 \tilde{p}_k + f(x_k)\tau,$$

where

$$f(x_k) = -\frac{d}{dx}V(x)\bigg|_{x=x_k}$$

is the force acting on the test particle between the kth and $(k+1)$th collisions. $\tau < \tau_0$ is the time elapsing after the kth collision. $\hat{x}_{k+1}$ and $\hat{p}_{k+1}$ are the coordinate and mechanical momentum of the test particle at time $k\tau_0 + \tau < (k+1)\tau_0$. Using our definition (1) of the characteristic function we can calculate its evolution between the kth and the $(k+1)$th collisions by means of the equation

$$C_k(l,h,T,\tau;x_0,p_0) = \int \frac{d\tilde{p}_k}{\sqrt{2\pi T m}} \exp\left(-\frac{\tilde{p}_k^2}{2mT}\right) \tilde{C}_k(l,h,T;x_0,p_0).$$

Here

$$\tilde{C}_k(l,h,T;x_0,p_0) = \left\langle \exp\left(i\mu_2\tilde{p}_k\frac{\tau l}{M} + ip_k^-\mu_1\frac{\tau l}{M} + ihf(x_k)\tau + ilx_k + i\mu_1 h p_k^- + i\mu_2 h\tilde{p}_k \right)\right\rangle_{k-1} \tag{25}$$

When $\tau = 0$, this is just the characteristic function just after the kth collision event as defined by Eq. (1).

It is emphasized that generally our characteristic function is not differentiable at times $t = k\tau_0$ when the collisions occur. However, considering its evolution between the collisions one may define the time derivative of the characteristic function as the limit

$$\frac{\partial\langle\exp(ixl+iph)\rangle_k}{\partial t} = \lim_{\tau_0\to 0}\frac{C_k(l,h,T,\tau_0;x_0,p_0) - C_k(l,h,T,\tau=0;x_0,p_0)}{\tau_0}. \tag{26}$$

It is clear from the discussion in the preceding section that the limit $\tau_0 \to 0$ can be taken only if simultaneously the ratio of masses $\varepsilon \to 0$ for a constant parameter $\gamma_L = 2\varepsilon/\tau_0$. The latter plays the role of the friction coefficient.

Integrating over $\tilde{p}_k$ in Eq. (25), for $\tau = \tau_0$, and expanding over l and h one gets

$$C_k(l,h,T,\tau_0;x_0,p_0) = \langle\exp(ilx_k + ihp_k^-)\rangle + \frac{il}{M}\langle p_k^-\exp(ilx+ihp_k^-)\rangle\tau_0 + ih\langle f(x_k)\exp(ilx+ihp_k^-)\rangle\tau_0 - 2ih\langle p_k^-\exp(ilx+ihp_k^-)\rangle\varepsilon - 2h^2TM\langle\exp(ilx+ihp_k^-)\rangle\varepsilon + \cdots.$$

Here we use $\mu_1 \to 1 - 2\varepsilon$ and $\mu_2^2 \to 4$. Then substituting this expression into Eq. (26) one arrives at the following equation for the time derivative of the characteristic function:

$$\frac{\partial\langle\exp(ixl+iph)\rangle_t}{\partial t} = ih\langle f(x)\exp(ixl+iph)\rangle_t + \frac{il}{M}\langle p\exp(ixl+iph)\rangle_t - T\gamma_L M h^2\langle\exp(ixl+iph)\rangle_t - ih\gamma_L\langle p\exp(ixl+iph)\rangle_t. \tag{27}$$

Keeping in mind that $p_k^- = p_k^+$ in the the limit $\varepsilon \to 0$ the notation $p = p_k^-$ is used. The averages in (27) mean integration over $(k-1) \to \infty$ momenta of colliding particles. The first two terms on the right-hand side (RHS) of Eq. (27) are due to the Taylor expansion in τ_0 and correspond to the evolution of the characteristic function due to the Newton deterministic motion of the test particle. The last two terms appear when expanding with respect

to ε and correspond to the contribution of the collisions.

In order to understand the meaning of this equation and its connection with the Kramers equation one has to consider the Fourier transform of our characteristic function

$$Q(x,v,t) = \int \frac{dl}{2\pi} \int \frac{dhM}{2\pi} \exp(-ilx - ipx) \times \langle \exp(ilx' + ihp') \rangle_t = \langle \delta(x - x')\delta(v - v') \rangle. \quad (28)$$

Keeping in mind that the averaging procedure in Eq. (28) is defined by the path integral obtained from (1) in the limit $\tau_0 \to 0$, can we say that the function $Q(x,v,t)$ is the probability density that *at the time* t the test particle wandering in the phase space visits the point with the coordinate x and the velocity $v = p/M$? If this is the case, one can replace the integration over all momenta of incident particles with the more conventional integration over phase space, weighted by a probability density $W(x,v,t)$, for which transition probabilities determine its evolution.

To check the equivalence of the two approaches, one has to make the Fourier transformation of Eq. (27), which results in

$$\frac{\partial Q(x,v,t)}{\partial t} = \left[-\frac{\partial}{\partial x} v + \frac{\partial}{\partial v} \left(v\gamma_L - \frac{f(x)}{M} \right) + \frac{\gamma_L T}{M} \frac{\partial^2}{\partial v^2} \right] Q(x,v,t). \quad (29)$$

The well-known Kramers equation (e.g., [9]), which is usually written for the probability density $W(x,v,t)$, is immediately recognized. The initial conditions for both probability densities coincide:

$$Q(x,v,t=0) = W(x,v,t=0) = \delta(x - x_0)\delta\left(v - \frac{p_0}{M}\right) \quad (30)$$

and their evolution is described by the same Kramers equation. Therefore

$$Q(x,v,t) = W(x,v,t) \quad (31)$$

at all times t.

It is worthwhile mentioning that the well-known problem of separation of friction force from fluctuating force and the consequences for the nonlinear Langevin equation discussed by Macdonald [13] and van Kampen [9] (Chap. 9) does not appear in our formulation. Our approach does not use such a separation at any step. As explained, our model for the nonlinear equation case turns out to be described well by the Kramers equation. This result is a direct consequence of our model rather than due to an ambiguous addition of a Gaussian white noise term to a nonlinear deterministic equation.

IV. NUMERICAL RESULTS

When the particle is situated in a nonlinear potential field an exact solution to the problem is rarely found. The subject of a stochastic motion in such fields is of great current interest [14]. Numerical solutions [15] are a common way to treat such problems. Here we use the collision process to simulate the Brownian type of motion.

The deterministic evolution of the particle during the time intervals τ_0 is obtained by solving numerically the Newton equations of motion. This was done using the leapfrog method with a time step satisfying $0.002 \leq \Delta t \leq 0.008 \ll \tau_0$. A double well potential (DWP) and an anharmonic oscillator are considered. The force field is given by $f(x) = -cx^3 + bx$ with $c = 1$, $b = 1$ for the DWP and with $c = 1$, $b = -1$ for the anharmonic oscillator.

First we have checked that the algorithm produces samples which agree well with the Maxwell-Boltzmann distribution. This was done for different mass ratios, temperatures, time intervals τ_0, and integration steps Δt by computing, for example, the time averaged energy of the test particle, and comparing this quantity with the energy computed directly from the Maxwell-Boltzmann distribution. The result gives good agreement between the two averaging procedures. We have also produced histograms which show that the algorithm is an excellent tool to produce the Maxwell-Boltzmann distribution. Being sure that the algorithm produces samples at thermal equilibrium, we may turn to dynamical features of the algorithm.

A. Dynamical properties

As shown above no relaxation to the thermal equilibrium occurs for the test particle in the harmonic potential whose frequency ω coincides with the period of kicks, $\omega\tau_0 = 2\pi$. An anharmonic potential is now considered. The corresponding averaged (temperature dependent) frequency of the test particle oscillations is

$$\langle \omega^2(T) \rangle = M^{-1} \left\langle \frac{\partial^2 V(x)}{\partial x^2} \right\rangle_T. \quad (32)$$

Here $\langle \rangle_T$ denotes averaging over the Boltzmann distribution.

This equation determines the characteristic oscillation period as $\langle t \rangle = 2\pi/\sqrt{\langle \omega^2 \rangle}$. The dynamics of the test particle close to thermal equilibrium will be studied assuming that the system is also close to the condition $\tau_0 \approx \langle t \rangle$. It is done by computing the correlation function

$$\xi(j) = \frac{\langle x(i)x(i+j) \rangle}{\langle x^2 \rangle_T}, \quad (33)$$

and time

$$t_{cor} = \tau_0 \sum_{j=0}^{\infty} \xi(j),$$

where i and j are indices of the collision events. The

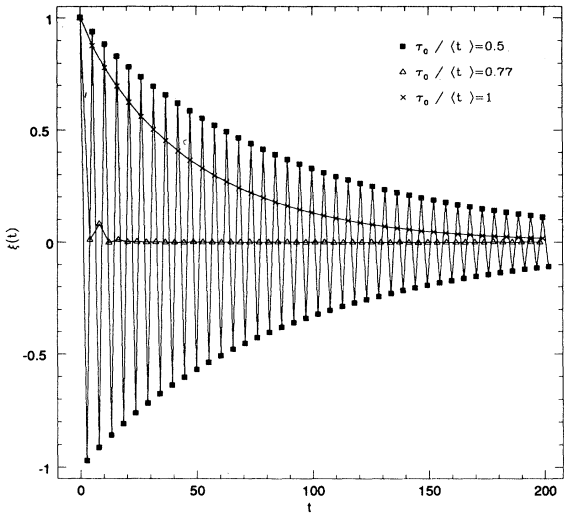

FIG. 4. Correlation functions are plotted for different time intervals τ_0 between collisions. Here we consider the anharmonic oscillator; the parameters of simulation are specified in the text.

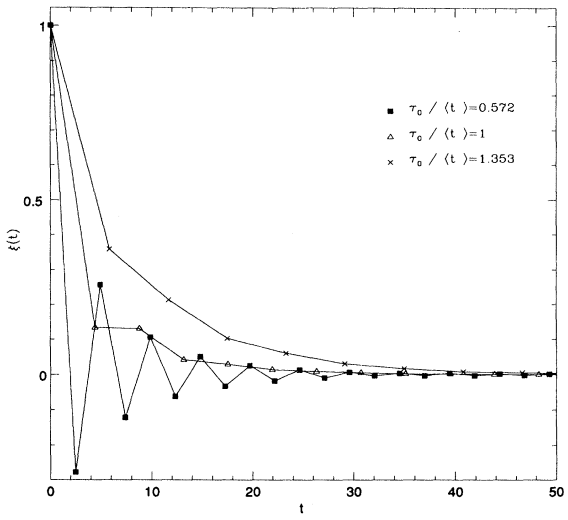

FIG. 6. Correlation functions are plotted for different time intervals τ_0 between collisions. Here we consider the DWP configuration; the parameters of simulation are specified in the text.

averaging in (33) is carried out both over the time (using 5000 event samples) and over 500 realizations. It is of interest to compute the dependence of these functions on temperature and on the time interval τ_0.

The slow relaxation is illustrated for the example of the force field $f(x) = -x^3 - x$, other parameters being $T = 0.2$, $\epsilon = 1$, and $\Delta t = 0.005$. Figure 4 shows how the correlation function varies with τ_0 so that the slow relaxation shows up when choosing τ_0 close to the averaged oscillation period. One can also observe strong oscillations of the correlation function when $\omega\tau = \pi$. These are due to sampling once to the left and once to the right of the central point of the oscillator. Figure 5 exhibits this phenomenon most distinctly by presenting the correlation time as a function of τ_0 for fixed temperature. The peak of this curve is situated very close to the estimate given by Eq. (32).

We have carried out these simulations also for the DWP configuration. The chosen temperature was $T = 1$, the mass ratio $\epsilon = 1$, and time step $\Delta t = 0.002$. Figure 6 shows the correlation function for various τ_0. Similarly to the anharmonic potential case, one observes the oscillations of the correlation function for $\tau_0/\langle t\rangle \simeq 0.5$. For the DWP case the peak in the correlation time (see Fig. 7) is shifted. Hence the rule (32) can give only a rough estimate for the location of the resonance. Due to the strong anharmonicity of the DWP, the correlation function in the DWP decreases more rapidly in comparison to the weakly anharmonic potential. Figure 7 shows

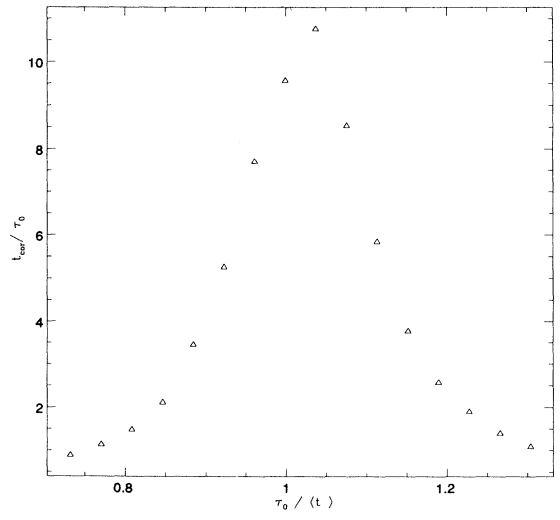

FIG. 5. Correlation time for the anharmonic oscillator, shown for different time intervals τ_0 between collisions.

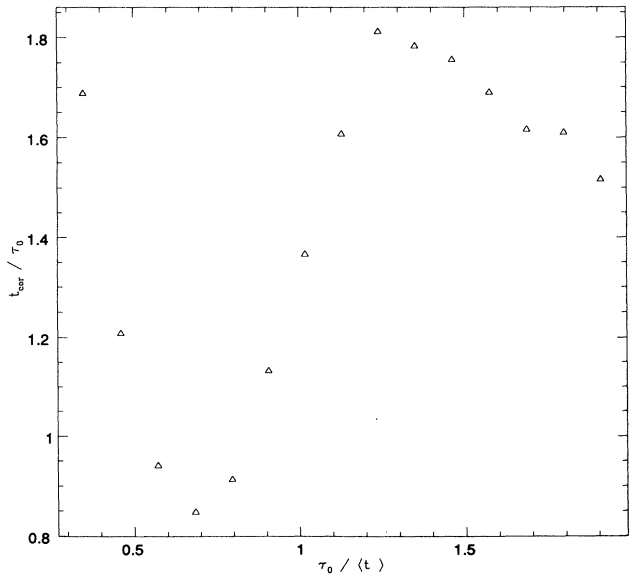

FIG. 7. Correlation time for the DWP configuration.

also an increase in the correlation time for small values of τ_0 when the motion is overdamped.

As a final remark we shall note that the results presented here are not sensitive to small changes in the time step Δt. Exactly the same simulations were carried out for the time step $\Delta t = 0.008$. The results for the correlation time varied only slightly, the maximal magnitude of these variation being 2%. We shall discuss further the dependence of the algorithm on the time step Δt in the next subsection.

B. Stability of paths

It is well known that a trajectory of a particle in a nonlinear potential field may be sensitive to small perturbations. Here the stability of the dynamics is considered with respect to variations of the integration step Δt. For this, two particles driven by an identical sequence of random collisions are studied. The initial conditions for the two particles are identical and so is the time step τ_0. It is clear that the departure of the trajectories of the two particles is due to small differences in the deterministic evolution. To measure this the normalized mean square distance $\langle r_{12}^2 \rangle = \langle (X_1 - X_2)^2 \rangle / \langle x^2 \rangle_T$ is defined.

It is found that a quantitative transition occurs for such dynamics which is sensitive to small changes of the time between collisions τ_0. This means that the value of $\langle r_{12}^2 \rangle$ may change by ten orders of magnitude when only slightly changing τ_0. Figure 8 exhibits the mean squared distance for three values of τ_0. The discretization time steps were chosen as $\Delta t_1 = 0.008$ and $\Delta t_2 = 0.002$, though other choices produce similar results. The averaging was carried out over 250 realizations. The figure shows the relative stability of the simulations when τ_0 is small.

We have also found the stationary value of $\langle r_{12}^2 \rangle$. This was done by averaging over both 250 realizations and 600 time steps. The dependence on τ_0 is shown in Fig. 9.

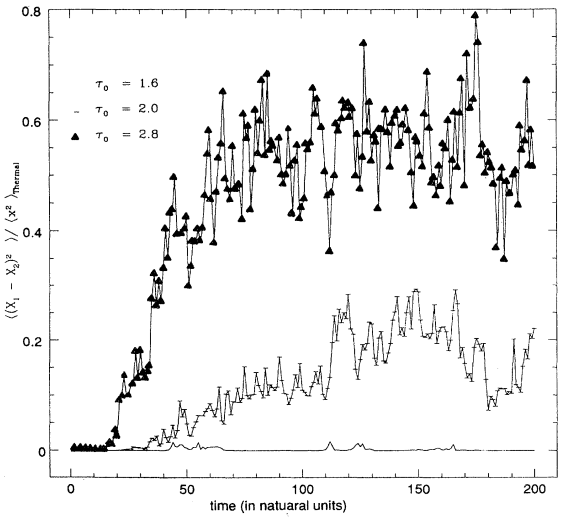

FIG. 8. The mean square distance as a function of time. Here $V(x) = \frac{x^4}{4} - \frac{x^2}{2}$, $\varepsilon = T = 1.0$.

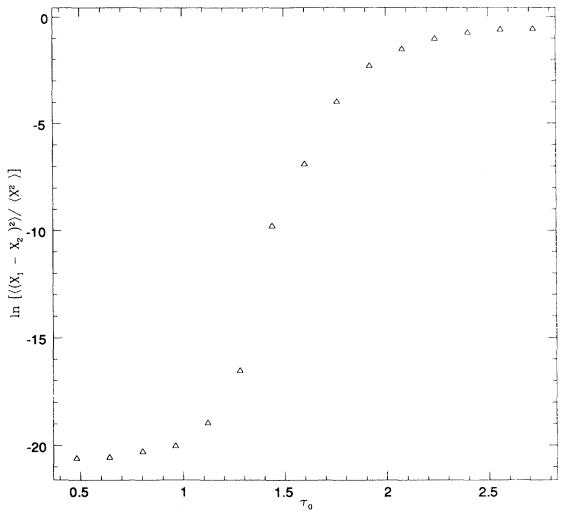

FIG. 9. Mean square distance as a function of τ_0. The parameters are given in Fig. 8.

This kind of transition is similar to the one found by Fahy and Hamann (FH) [5]. They found that when two particles are driven by the same sequence of random collisions their trajectories may become identical. The transition is from a chaotic behavior (trajectories do not become identical) for long intervals between collision events to a nonchaotic behavior (trajectories become identical) for short intervals. However, the perturbation imposed on the two paths, in our simulations, is not due to different initial conditions given to the two particles. Rather, it is due to the difference in the discretization step chosen for the two trajectories. Hence in our simulation, even if the two particles occupy exactly the same point in phase space, their paths will separate.

To understand this, consider the two particles initially situated at the same point in phase space. Due to the small difference in the discretization step the particle trajectories will depart (even for small values of τ_0). After the two particles have separated slightly, we show why they tend to contract for small values of τ_0. Expanding the coordinate in τ_0 one gets

$$\frac{x_1(\tau_0) - x_2(\tau_0)}{x_1(0) - x_2(0)} = 1 - \frac{\tau_0^2}{2M} \frac{\partial^2 V}{\partial x^2}. \tag{34}$$

It is clear that such an expansion is valid only when the dynamics are approximately described by Newton's equations (i.e., assuming Δt_i are small enough). As pointed out by FH the second term in (34) is for bounded systems, on the average positive. Hence the particles will effectively attract each other.

V. CONCLUSIONS

A description of the motion of a particle coupled to a "heat bath" is presented. This stochastic motion serves to generate samples obeying Maxwell-Boltzmann statistics. The particle statistical properties are determined

by an integration scheme (path integral) over all incident particles. This procedure is similar to the Wiener representation of the random walk problem [16]. There the inertial effects of the particle's motion are not considered. The path integral method suggested here is particularly useful far from the diffusion limit. In this case the motion is described neither by a differential (i.e., Fokker-Planck) equation nor by an integro-differential equation.

Considering the limit of *both the time between collision and the mass ratio* (bath to test particle) *tending to zero*, we arrive at the standard results derived from the phenomenological Langevin equation. Several cases of finite time between collision and ratio of masses are considered, when the description does not necessarily coincide with that of the Langevin equation.

This allows us also to study whether ergodicity holds for the particular systems and find particular situations when it is broken down. This happens when $\omega\tau_0 = n\pi$ where ω is the frequency of a harmonic background potential. For anharmonic potentials the frequency of motion is a function of the amplitude; hence one expects ergodicity to hold always. Even so, choosing τ_0 close to an averaged period (now depending on the amplitude and hence the temperature) of the anharmonic background potential may lead to slowing down of the relaxation. This and the fact that choosing τ_0 too small leads to a highly overdamped motion restrict the choice of τ_0. We therefore may conclude that the choice of τ_0 should be made with care. A possible way to avoid such complications is to choose τ_0 from an exponential distribution.

We have also found a sharp transition for the sensitivity of the paths to small changes of the integration step Δt. For small values of τ_0 the paths are not sensitive to this parameter, while beyond a critical value of τ_0 the trajectories are not stable. This means that the path for large τ_0 depends on the integration step, even if it is very small. In this case, as for many other numerical procedures, one may extract numerical results only after checking that the result is insensitive to this integration step.

ACKNOWLEDGMENTS

The authors are thankful to Professor Z. Schuss for fruitful discussions. The work was supported by the German-Israeli Foundation for Scientific Research and Development, Grant No. I-140-125.7/89 and by Sonderforschungsbereich 262.

[1] S. Duane, A.D. Kennedy, B. Pendelton, and D. Roweth, Phys. Lett. B **195**, 216 (1987).
[2] H.C. Andersen, J. Chem. Phys. **72**, 2384 (1980).
[3] J.A. Montgomery, D. Chandler, and B. Berne, J. Chem. Phys. **70**, 4056 (1979).
[4] M. Borkovec, J.E. Straub, and B.J. Berne, J. Chem. Phys. **85**, 146 (1986).
[5] S. Fahy and D.R. Hamann, Phys. Rev. Lett. **69**, 76 (1992).
[6] B. Mehling, D.W. Heermann, and B.M. Forrest, Phys. Rev. B **45**, 679 (1992).
[7] R. Mannella, in *Noise in Nonlinear Dynamical Systems*, edited by F. Moss and P.V.E. McClintock (Cambridge University Press, Cambridge, England, 1989), Vol. 3, pp. 189–221.
[8] A. Greiner, W. Strittmatter, and J. Honerkamp, J. Stat. Phys. **51**, 109 (1988).
[9] N.G. van Kampen, *Stochastic Processes in Physics and Chemistry* (North-Holland, Amsterdam, 1981).
[10] M.R. Hoare, Adv. Chem. Phys. **XX**, 135 (1971).
[11] S. Chandrasekhar, Rev. Mod. Phys. **15**, 1 (1943).
[12] R.P. Feynman and A.R. Hibbs, *Quantum Mechanics and Path Integration* (McGraw-Hill, New York, 1965).
[13] D.K.C. MacDonald, Phys. Rev. **108**, 541 (1957).
[14] *Noise in Nonlinear Dynamical Systems*, edited by F. Moss and P.V.E McClintock (Cambridge University Press, Cambridge, England, 1989), Vols. 1–3.
[15] J.M. Sancho, M. San Miguel, S.L. Katz, and J.D. Gunton, Phys. Rev. A. **26**, 1589 (1982).
[16] I.M. Gel'fand and A.M. Yaglom, J. Math. Phys. **1**, 48 (1960).